ENVIRONMENTAL RESEARCH
LETTERS

LETTER • **OPEN ACCESS**

Attribution of the impacts of the 2008 flooding in Cedar Rapids (Iowa) to anthropogenic forcing

To cite this article: Gabriele Villarini *et al* 2020 *Environ. Res. Lett.* **15** 114057

Environmental Research Letters

LETTER

Attribution of the impacts of the 2008 flooding in Cedar Rapids (Iowa) to anthropogenic forcing

Gabriele Villarini[1], Wei Zhang[1], Felipe Quintero[1], Witold F Krajewski[1] and Gabriel A Vecchi[2,3]

[1] IIHR—Hydroscience & Engineering, The University of Iowa, Iowa City, IA 52242, United States of America
[2] Department of Geosciences, Princeton University, Princeton, NJ, United States of America
[3] Princeton Environmental Institute, Princeton University, Princeton, NJ, United States of America

E-mail: gabriele-villarini@uiowa.edu

Keywords: attribution, flood, global warming, CESM, Iowa, climate change

Supplementary material for this article is available online

OPEN ACCESS

RECEIVED
31 July 2020

REVISED
13 October 2020

ACCEPTED FOR PUBLICATION
29 October 2020

PUBLISHED
24 November 2020

Abstract

The City of Cedar Rapids was significantly affected by the June 2008 flood. However, little is known about the role anthropogenic warming during this event, not only in terms of hydrologic response but also of impacts. Here we use a continuous distributed hydrologic model forced with precipitation with and without external forcing and show that the impacts of this flood were likely magnified because of increased anthropogenic warming; compared to the baseline scenario with the external forcing removed, this event was ~1.28-fold larger in flood extent, an approximate 3.4-time larger in the number of affected buildings, and an estimated 5.8- and 7.1-time larger in structural and content damage, respectively. While much of the effort up to this point has focused on the attribution of the physical hazard, our results highlight the cascading increase of the contribution of the external forcing (mainly from anthropogenic forcing) moving from hazard to human impacts.

1. Introduction

The U.S. Midwest is no stranger to flooding: this is an area of the country that has been plagued by large floods, with their frequency increasing over the recent decades (e.g. Mallakpour and Villarini 2015, Neri *et al* 2019). Specific flood events can leave long-lasting impacts on the well-being of those affected, especially when these events are experienced multiple times over the years: floods like those that occurred in 1993, 2008, 2011, 2017 and, more recently in 2019, have been responsible for several fatalities and many billion dollars in economic damage.

It has now been over 12 years since the 2008 flooding event (e.g. NWS 2009, Mutel 2010, Zogg 2014, Cedar Rapids 2020), which was characterized by discharge values much larger than those recorded in 1993 across large areas of Iowa (Smith *et al* 2013). This event remains by far the largest one in the 117-year record. To put it in context, with a peak discharge of 140 000 $ft^3\ s^{-1}$, it was twice as large as the 1993 peak (71 000 $ft^3\ s^{-1}$) and almost twice as large as the second largest value (81 600 $ft^3\ s^{-1}$; September 2016). The City of Cedar Rapids was significantly impacted by this event, with over 10 000 (of ~127 000) residents estimated to have been displaced because of the flood and 14% of the city area impacted by floodwaters, but fortunately not in terms of fatalities. The event replaced the 1993 flood as a reference for 'before' and 'after' in many aspects of life for the residents of Eastern Iowa. Despite a decade of significant progress in flood mitigation preparedness (Krajewski *et al* 2017), several questions still remain unanswered regarding the potential role external forcing may have played in the rainfall during the 2008 event. Was this event altered by the multi-decadal climate response to these external forcing? This type of attribution question has received substantial attention in the literature, with most of the hydroclimatological focus on rainfall amounts (e.g. Risser and Wehner 2017, Van Oldenborgh *et al* 2017, Wiel *et al* 2017, Otto *et al* 2018, Philip *et al* 2019), with fewer studies assessing the role of external forcing to specific flood events (e.g. Pall *et al* 2011, Schaller *et al* 2016). Even less is known about the contribution of global warming to impacts. In this study we seek to quantify the role that anthropogenic warming effects played not

only in terms of hazard (i.e. heavy precipitation and flooding), but also regarding impacts, intended here to include flood extent and inundated areas, number of affected buildings, and structural and content damage.

2. Data and methods

The observed rainfall data are obtained from the Stage IV quantitative precipitation estimates (QPEs) products over the continental United State (CONUS) (Lin and Mitchell 2005) released by the National Centers for Environmental Prediction (NCEP). Stage IV has been shown to have low bias when compared to rain gauge measurements in the state of Iowa (Seo *et al* 2018). The discharge data are obtained from the United States Geological Survey (USGS).

The six-hour initial and boundary conditions used to simulate the extreme event that occurred during June 6–12 2008 are obtained from the ERA-Interim reanalysis data released by the European Centre for Medium-Range Weather Forecasts (ECMWF), at a spatial resolution of ∼0.7 degree (Dee *et al* 2011). In addition to ERA-Interim, we performed dynamical downscaling using other reanalysis data including the North American Regional Reanalysis (NARR), the Japanese 55-year Reanalysis (JRA-55), and the NCEP Climate Forecast System Version 2 (CFSv2) 6-hourly products. The ERA-Interim data performed the best in reproducing the observed precipitation with respect to Stage IV.

The Weather Research and Forecasting (WRF) model is used to perform the dynamical downscaling of the extreme precipitation event responsible for the flooding during June 2008. We used the Advanced Research WRF (WRF-ARW) for the simulations, and performed the experiments in two domains with two-way nesting with 12 km and 4 km for the outer and inner domain, respectively (supplementary figure 1 (available online at https://stacks.iop.org/ERL/15/114057/mmedia)). The main parameterization schemes are listed in supplementary table 1. The setting of parameterization schemes for WRF ARW in this study has been used in previous studies (e.g. Talbot *et al* 2012, Li *et al* 2013, El-Samra *et al* 2017, Zhang *et al* 2018). In particular, the previous WRF tests for this setting can be found in Li *et al* (2013) and Talbot *et al* (2012). Although there is still uncertainty in the simulation of WRF experiments due to parameterization schemes, the current setting is expected to be suitable for the simulation of heavy precipitation processes. The WRF simulation is integrated from June 6th 00:00:00 to June 13th 00:00:00, 2008.

We follow the 'pseudo global warming' method used in the literature to examine the role of global warming in shaping weather events (e.g. Schär *et al* 1996, Rasmussen *et al* 2011). This approach applies a change associated with global warming to the input variables of the original initial and boundary conditions (e.g. winds, humidity and temperature) based on reanalysis data. The 'global warming' change can be obtained by subtracting the input variables in the historical experiments from future projections. Regional model experiments have indicated that the removal of the historical trend based on the Coupled Model Intercomparison Project Phase 5 (CMIP5) models in the forcing data can cause substantially reduced precipitation during a flood event that affected India during June 2013 (Cho *et al* 2016). Here we use a strategy similar to that used in Cho *et al* (2016), with the forcing variables' trends computed from the large initial condition ensemble experiments performed with the Community Earth System Model developed by National Center for Atmospheric Research (NCAR CESM) (Kay *et al* 2015). Cho *et al* (2016) performed Control and No-trend experiments to assess the impacts of global warming (i.e. Control minus No-trend). The Control experiment is forced by the initial and boundary conditions from reanalysis data, and the linear climate trends in all initial and boundary condition variables are removed in the No-trend experiment. More specifically, we run two sets of experiments: the 'Original' and 'Detrend' experiments during the time period of interest and based on the average of 42 members. In the 'Original' experiment, we feed the initial and boundary conditions from ERA-Interim data directly into WRF-ARW. In contrast, the 'Detrend' experiments use the initial and boundary conditions of ERA-Interim but detrend the three-dimensional zonal and meridional wind, geopotential height, and temperature based on the trends computed from the CESM large-ensemble experiments to quantify the impacts of external forcing. The trends are computed using linear regression for the month of June over the base period 1979–2005. We did not remove the trend in relative humidity to avoid the risk of having values larger than 100%. Although removing trend in the temperature field plays a major role in driving changes in precipitation in the study area, we cannot exclude potential impacts of external forcing on other variables (e.g. zonal and meridional winds). Therefore, we also remove the trends in the three-dimensional zonal and meridional wind, and geopotential height.

The three-dimension trends (e.g. degree/year for temperature) of the four variables are vertically and horizontally interpolated into the levels and grids of ERA-Interim before we subtract the trends from the initial and boundary conditions from ERA-Interim. Supplementary figure 2 shows the trends of the bottom-level temperature based on the 42-member large-ensemble CESM experiments and the associated signal-to-noise ratio. The subtraction of the 'Detrend' experiment from the 'Original' one

represents the impacts of externally-forced trends on this weather event. The trends based on the large ensemble experiments can quantify the trends due to external forcing because natural variability in different ensembles can cancel each other off (e.g. Cho *et al* 2016). The trends in the four variables from CESM are subtracted from the four variables from ERA-Interim reanalysis data, which provide initial and boundary conditions for the WRF model. The uncertainties associated with the externally-forced signal are computed using the 95% confidence intervals on the estimated trend coefficients. The 95% confidence intervals on the estimated trend coefficients are defined based on the linear regression model:

$$Y_i = \beta_0 + \beta_1 X_i + \varepsilon_i \quad (1)$$

where Y_i is the dependent variable, X_i is the independent variable (i.e. time), β_0 is the intercept, β_1 is the slope/trend and ε_i is the random error.

The 95% CI is calculated based on the equation below:

$$\widehat{\beta_1} - t_{\alpha/2,n-2}\sqrt{\frac{\hat{\sigma}^2}{S_{xx}}} \leqslant \beta_1 \leqslant \widehat{\beta_1} + t_{\alpha/2,n-2}\sqrt{\frac{\hat{\sigma}^2}{S_{xx}}} \quad (2)$$

where $\widehat{\beta_1}$ is the estimated trend, $t_{\alpha/2,\,n-2}$ is the t value for the significance level (here 0.05) with n being the sample size, and S_{xx} and $\hat{\sigma}^2$ are defined as:

$$S_{xx} = \sum_{i=1}^{n} (x_i - \bar{x})^2. \quad (3)$$

$$\hat{\sigma}^2 = \frac{\sum_{i-1}^{n} (y_i - \hat{y}_i)^2}{n-2}. \quad (4)$$

For the hydrologic simulations, we used the model developed by the Iowa Flood Center (IFC), which produces real-time streamflow predictions for all the communities in the state of Iowa using a continuous distributed hydrologic model known as Hillslope-Link Model (Quintero *et al* 2016, Krajewski *et al* 2017). The model is calibration-free i.e. a common configuration of parameters determined *a priori* applies for all the model inputs, and no adjustments are made for particular basins. The model uses hillslopes and channel links as the primary units for landscape decomposition where the hydrologic processes are modeled. Rainfall conversion to runoff is modeled through accounting for soil moisture changes at the hillslopes. Channel routing is based on a non-linear representation of water velocity that considers the discharge amount as well as the upstream drainage area (Gupta *et al* 2010, Ghimire *et al* 2018). Mathematically, the model represents a large system of ordinary differential equations organized following river network topology. The IFC also developed an efficient numerical solver suitable for High Performance Computing architecture (Small *et al* 2013). The hydrologic simulations obtained with the configuration of the Hillslope-Link Model were extensively validated over a period of seven years and showed good performance when using Stage IV data as rainfall forcing (Quintero *et al* 2020). We initialized the states of the hydrologic model using the conditions observed for discharge and soil moisture for June 6th 2008.

For the estimation of economic losses due to flood we used several sources of data. Inundation maps were developed by the IFC for the city of Cedar Rapids using HEC-RAS to estimate water surface elevations in the river channels and floodplain that results from discharge estimates of different return periods; water surface data were intersected with a 1-m DEM to calculate the flood extents. The inundation maps contain detailed urban flooding analysis that takes into account location and heights of the buildings (Gilles *et al* 2012). Depth-damage functions and detailed building data are available from U.S. Army Corps of Engineers (USACE), Federal Emergency Management Agency (FEMA) and property tax assessors (e.g. Scawthorn *et al* 2006, Yildirim and Demir 2019). These datasets were used to calculate the dollar amount losses based on the content and structural value of individual properties.

3. Results

This attribution study involves a combination of observations, and hydrologic, atmospheric and climate modeling. Although flooding and extreme rainfall are not the same thing (e.g. Ivancic and Shaw 2015), heavy rainfall represents the basic ingredient for this flood event; the soil was already saturated because of extensive precipitation earlier in the spring. As discussed in Krajewski and Mantilla (2010), this region experienced one of the snowiest winters; even though the heavy snow was not directly responsible to this event, it left the ground saturated. In late May, a number of storms trailed over Iowa, with rainfall falling on the already saturated ground (e.g. Coleman and Budikova 2010, Krajewski and Mantilla 2010). The conditions were primed for the heavy rainfall across the Cedar River during 6–12 June (figure 1). During 6–8 June, the rainfall was concentrated in the upper part of the basin; as the water flowed downstream and the peak propagated downstream towards the City of Cedar Rapids, the areas with heavy rainfall seemed to follow the crest, with much of the rainfall concentrated in the middle and lower parts of the basin. The amount and timing of the precipitation translated to the observed discharge time series (figure 2), which is well reproduced both in terms of timing and magnitude by the IFC hydrologic model forced with radar-based rainfall estimates, and initialized with soil saturated conditions. For this

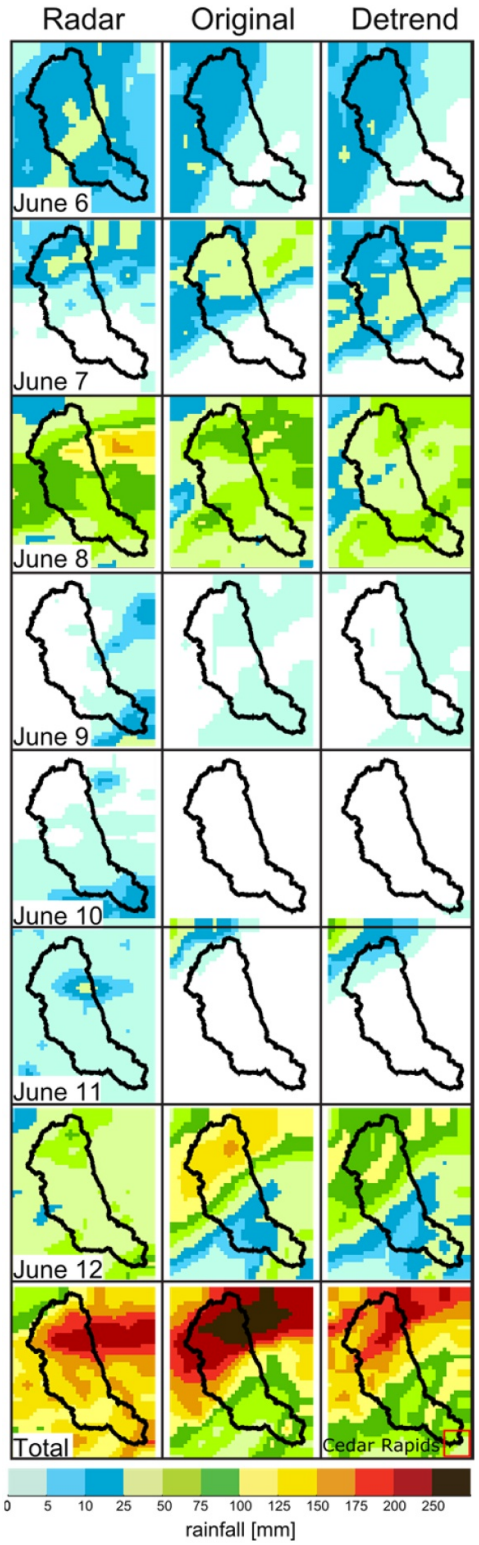

Figure 1. Comparison between observed and modeled precipitation. Daily rainfall maps for 6–12 June 2018 as well as their accumulation in (left column) observations, and based on the atmospheric model before (middle column) and after (right column) removing the externally-forced climatic effects. The black polygon in each map represents the Cedar River at Cedar Rapids. The red square in the bottom right map indicates the location of the city of Cedar Rapids.

event the IFC hydrologic model is able to reproduce well the observations.

Before quantifying the role of external forcing on this flood event, we examined whether the hydrologic response forced by the dynamically downscaled outputs was similar to the observed one (figure 1 and supplementary figure 3). Although not 'perfect' in terms of precipitation, the atmospheric model can reproduce the overall daily rainfall amounts, with good agreement with observed the basin-averaged total rainfall (supplementary figure 3). A notable difference is related to the timing and the detailed regional distribution of the precipitation, with large amounts concentrated in the upper part of the basin. Therefore, from a hydrologic perspective we would expect that the agreement in total rainfall would drive total discharge volumes comparable to observations, while the delay and geographic shift to the upper part of the basin would delay the flood peak by few days. As shown in figure 2, the overall magnitude of the modeled peak is very similar to the observed one (whether when compared against gauge measured discharge or from that estimated by forcing the hydrologic model with radar-rainfall estimates), with the main difference being that the modeled peak is delayed by approximately four days. The focus here is on damages arising from the large flood peak in this event, and not the details in the timing of that peak.

The results in figures 1–2 indicate that the combined reanalysis-hydrologic model system can simulate the rainfall and hydrologic response to this rainfall event in a satisfactory manner, encouraging us to move towards quantifying the associated external component. In our perturbation experiments which focused on the thermal-dynamic effects, we did not find evidence that anthropogenic warming led to a marked change in where and when the higher rainfall occurred (comparing the middle and right panels in figure 1) but had mostly an effect on the magnitude, leading to larger amounts (supplementary figure S3). These impacts are then expected to manifest themselves in a hydrograph that mimics one forced with the raw model outputs, even though the peaks have smaller magnitudes (i.e. the largest peak is lower by 2 m). Mounting evidence has shown that the multi-decadal increase in surface temperature can be mainly attributed to anthropogenic forcing, rather than natural forcing (e.g. volcanic eruption and solar irradiance) and internal variability (Flato *et al* 2014). The increasing atmospheric temperature plays an important role in driving changes in extreme precipitation events, in part due to increasing atmospheric moisture following the Clausius-Clapeyron (C-C) relation (e.g. Held and Soden 2006, Donat *et al* 2016). We find that the flood peak at Cedar Rapids was approximately 2 m higher because of anthropogenic warming, an amount that leads to statistically different results at the 5% significance level (figure 2).

Having assessed that anthropogenic warming mainly enhanced the magnitude (or equivalently the

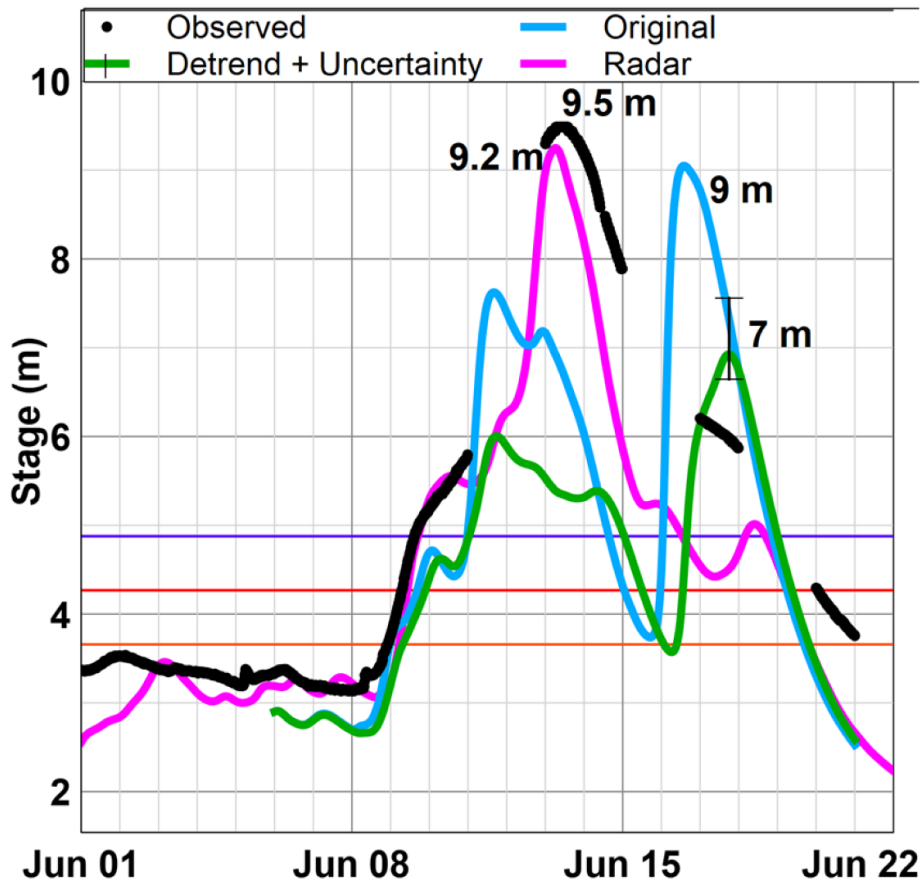

Figure 2. Time series of the observed and modeled discharge. The black line represents the observations, with the gaps in the time series due to the stream gage not functioning. The magenta line shows the time series obtained forcing the hydrologic model with radar-based rainfall; the blue and green lines show the modeled discharge when forced with downscaled precipitation before and after removing (together with the 95%-confidence intervals) the effects of the external forcing, respectively. The horizontal lines represent the minor (orange), moderate (red) and major (purple) flood levels established by the National Weather Service.

Table 1. Summary of the impacts of external forcing on flood extent, number of affected buildings, and economic losses. The results for 'Original' are based on the initial and boundary conditions from ERA-Interim, which are fed directly into WRF-ARW. In contrast, the results for 'Detrend' are based on the initial and boundary conditions of ERA-Interim but detrended based on the trends computed from the CESM large-ensemble experiments. In both cases, the WRF-ARW outputs are used as inputs for the hydrologic model. The column 'Ratio' shows the ratio between the 'Original' and 'Detrend' scenarios. The results in the square brackets represent the 95%-confidence limits.

	Original (9 m)	Detrend (7 m)	Ratio
Area (km^2)	51.2	39.9 [36.5; 43.5]	1.28 [1.18; 1.40]
Affected Buildings (#)	3703	1089 [677; 2068]	3.40 [1.79; 5.47]
Structure Damage (USD)	35 977 020	6 169 376 [4 299 928; 10 864 656]	5.83 [3.31; 8.37]
Content Damage (USD)	83 675 455	11 851 114 [8 331 197; 21 932 535]	7.07 [3.82; 10.04]

probability) of the meteorological hazard, we now seek to propagate this information through to evaluate the major role of this warming from discharge, to flood extent, to economic impacts (table 1). Figure 3 shows the flood extent in Cedar Rapids at 7 and 9 m, and the difference in flooding that can be mainly attributed to anthropogenic warming. Based on our results, the extent of the inundated areas is 1.28 times larger (compare 51.2 km^2 to 39.9 km^2; table 1), with large areas of Cedar Rapids that would not have been inundated. Because housing and wealth are not distributed uniformly across the affected area, the impacts are not going to be necessarily of the same order of magnitude. As shown in table 1, the number of affected building increased from an expected ∼1100 to ∼3700, a 3.4-fold increase. Nevertheless, given the type of buildings and their expected content, we can attribute mainly to anthropogenic warming an estimated 5.8-fold and 7.1-fold increase in the structural and content damage, respectively. These non-linear effects are associated with the non-linear relationships that characterize vulnerability curves, which relate water depth to economic damage (Scawthorn *et al* 2006).

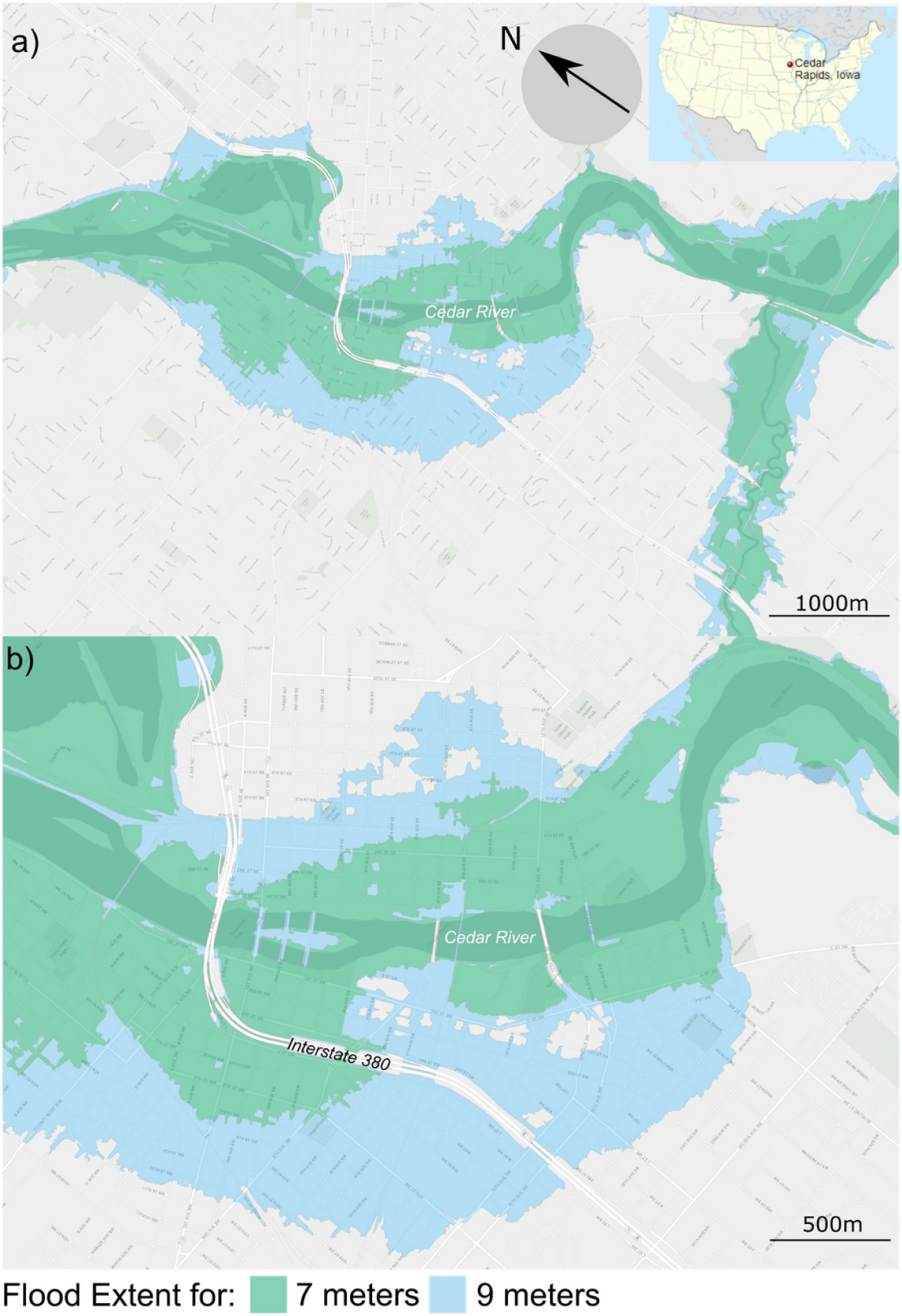

Figure 3. Comparison of the flood extent including or not the role of anthropogenic warming. The blue (green) areas represent the flood inundation extent for a stage equal to 9 (7) m, with the visible blue areas reflecting the inundation extent that can be attributed to external forcing. The top panel shows the Cedar River at Cedar Rapids, while the bottom panel focuses on downtown Cedar Rapids.

4. Conclusions

This study presents a novel framework to quantitatively assess the role of anthropogenic forcing in the context of the socio-economic impacts of the 2008 flooding in Cedar Rapids. We find that the anthropogenic warming-driven changes in water level led to a cascade of increasing impacts when one moves

from hydrological to societal and economic impacts. More specifically, a 2-m difference in peak streamflow (1.28-fold increase from 7 m to 9 m) led to an approximately 1.28-fold increase in inundated areas; however, when one considers economic losses, the impact grows to 7 times. These numbers should not be interpreted in an absolute sense, but rather relative to the flood peak and the topography of the affected area: a difference of 2 m resulting in water still being within the banks would have not led to any damage; moreover, the impacts would have been different in areas characterized by higher elevation on the river banks (i.e. compare the flood inundation extent differences close to the urban core of Cedar Rapids and more downstream; figure 3). Studies of this kind will allow us to move away from just the hazard attribution to their impacts, providing basic information that could inform policy changes in light of the economic impacts of climate change.

It is essential to note that this flood event and its impacts are not solely attributable to anthropogenic warming, but rather that this warming modified the amplitude and probability of this event. As shown by the flood inundation map, most of Cedar Rapids would have been flooded even after we removed the radiatively-forced anthropogenic warming. Our findings are based on assumptions related to the way that external drivers (mainly the anthropogenic component) affected the climate system, and the numbers could be slightly different depending on uncertainties in the trend estimation, hence they should be considered as estimates. We also quantified different sources of uncertainties associated with our approach. On the one hand, we found that the uncertainties due to the anthropogenic forcing are relatively small (table 1, figure 2 and supplementary figure 3) compared to its signal (results are significant at the 5% level). On the other hand, the noise associated with internal variability is large (supplementary figure 3). Using the large ensemble runs by the CESM we are able to isolate the externally forced signal, and our study highlights the importance of this type of simulations in making statements about the major role of anthropogenic warming.

Acknowledgments

This material is based in part upon work supported by the U.S. Army Corps of Engineers' Institute for Water Resources (IWR), IIHR—Hydroscience & Engineering, and the Iowa Flood Center. The CESM large ensemble run can be obtained via the link http://www.cesm.ucar.edu/projects/community-projects/LENS/data-sets.html. ERA-Interim data set is obtained from the website of ECMWF (https://www.ecmwf.int/en/forecasts/datasets/reanalysis-datasets/era-interim). Stage IV precipitation data can be obtained from https://data.eol.ucar.edu/dataset/21.093. USGS data are available through the USGS's National Water Information System (https://waterdata.usgs.gov/nwis). The flood inundation maps and flood damage are available from the Iowa Flood Information System (http://ifis.iowafloodcenter.org/ifis/en/).

ORCID iDs

Gabriele Villarini https://orcid.org/0000-0001-9566-2370
Wei Zhang https://orcid.org/0000-0001-8134-6908

References

Cedar Rapids 2020 Flood of 2008 facts & statistics Accessed: 12 June 2020 (available at: http://www.cedar-rapids.org/discover_cedar_rapids/flood_of_2008/2008_flood_facts.php#:~:text=On%20June%2013%2C%202008%2C%20the,record%20reached%20only%2020%20feet.&text=This%20monumental%20flood%20impacted%207%2C198,and%20damaged%20310%20City%20facilities)

Cho C, Li R, Wang S-Y, Yoon J-H and Gillies R R 2016 Anthropogenic footprint of climate change in the June 2013 northern India flood *Clim. Dyn.* **46** 797–805

Coleman J S M and Budikova D 2010 Atmospheric aspects of the 2008 Midwest floods: A repeat of 1993? *Int. J. Climatol.* **30** 1645–67

Dee D P, Uppala S, Simmons A, Berrisford P, Poli P, Kobayashi S, Andrae U, Balmaseda M, Balsamo G and Bauer D P 2011 The ERA-Interim reanalysis: configuration and performance of the data assimilation system *Q. J. R. Meteorolog. Soc.* **137** 553–97

Donat M G, Lowry A L, Alexander L V, O'Gorman P A and Maher N 2016 More extreme precipitation in the world's dry and wet regions *Nat. Clim. Change* **6** 508

El-Samra R, Bou-Zeid E, Bangalath H K, Stenchikov G and El-Fadel M 2017 Future intensification of hydro-meteorological extremes: downscaling using the weather research and forecasting model *Clim. Dyn.* **49** 3765–85

Flato G, Marotzke J, Abiodun B, Braconnot P, Chou S C, Collins W, Cox P, Driouech F, Emori S and Eyring V 2014 Evaluation of climate models *Climate change 2013: the physical science basis. Contribution of Working Group I to the Fifth Assessment Report of the Intergovernmental Panel on Climate Change* (Cambridge University Press) pp 741–866

Ghimire G R, Krajewski W F and Mantilla R 2018 A power law model for river flow velocity in Iowa Basins *JAWRA J. Am. Water Resour. Assoc.* **54** 1055–67

Gilles D, Young N, Schroeder H, Piotrowski J and Chang Y-J 2012 Inundation mapping initiatives of the Iowa Flood Center: statewide coverage and detailed urban flooding analysis *Water* **4** 85–106

Gupta V K, Mantilla R, Troutman B M, Dawdy D and Krajewski W F 2010 Generalizing a nonlinear geophysical flood theory to medium-sized river networks *Geophys. Res. Lett.* **37** L11402

Held I M and Soden B J 2006 Robust responses of the hydrological cycle to global warming *J. Clim.* **19** 5686–99

Ivancic T J and Shaw S B 2015 Examining why trends in very heavy precipitation should not be mistaken for trends in very high river discharge *Clim. Change* **133** 681–93

Kay J E, Deser C, Phillips A, Mai A, Hannay C, Strand G, Arblaster J M, Bates S, Danabasoglu G and Edwards J 2015 The community earth system model (CESM) large ensemble project: A community resource for studying climate change in the presence of internal climate variability *Bull. Am. Meteorol. Soc.* **96** 1333–49

Krajewski W F, Ceynar D, Demir I, Goska R, Kruger A, Langel C, Mantilla R, Niemeier J, Quintero F and Seo B-C 2017 Real-time flood forecasting and information system for the state of Iowa *Bull. Am. Meteorol. Soc.* **98** 539–54

Krajewski W F and Mantilla R 2010 Why were the 2008 floods so large? *A Watershed Year: Anatomy of the Iowa Floods of 2008* C F Mutel ed (Iowa City, IO: University of Iowa Press) pp 19–30

Li D, Bou-Zeid E, Baeck M L, Jessup S and Smith J A 2013 Modeling land surface processes and heavy rainfall in urban environments: sensitivity to urban surface representations *J. Hydrometeorol.* **14** 1098–118

Lin Y and Mitchell K E 2005 1.2 the NCEP stage II/IV hourly precipitation analyses: development and applications *19th Conf. Hydrology* (San Diego, CA: American Meteorological Society)

Mallakpour I and Villarini G 2015 The changing nature of flooding across the central United States *Nat. Clim. Change* **5** 250

Mutel C F 2010 *A Watershed Year: Anatomy of the Iowa Floods of 2008* (Iowa City, IO: University of Iowa Press)

Neri A, Villarini G, Slater L J and Napolitano F 2019 On the statistical attribution of the frequency of flood events across the US Midwest *Adv. Water Resour.* **127** 225–36

NWS 2009 Central United States flooding of June 2008 https://www.weather.gov/media/publications/assessments/central_flooding09.pdf

Otto F E, van der Wiel K, van Oldenborgh G J, Philip S, Kew S F, Uhe P and Cullen H 2018 Climate change increases the probability of heavy rains in Northern England/Southern Scotland like those of storm Desmond—a real-time event attribution revisited *Environ. Res. Lett.* **13** 024006

Pall P, Aina T, Stone D A, Stott P A, Nozawa T, Hilberts A G, Lohmann D and Allen M R 2011 Anthropogenic greenhouse gas contribution to flood risk in England and Wales in autumn 2000 *Nature* **470** 382

Philip S, Sparrow S, Kew S, Van Der Weil K, Wanders N, Singh R, Hassan A, Mohammed K, Javid H and Haustein K 2019 Attributing the 2017 Bangladesh floods from meteorological and hydrological perspectives *Hydrol. Earth Syst. Sci.* **23** 1409–29

Quintero F, Krajewski W F, Mantilla R, Small S and Seo B-C 2016 A spatial–dynamical framework for evaluation of satellite rainfall products for flood prediction *J. Hydrometeorol.* **17** 2137–54

Quintero F, Krajewski W F, Seo B-C and Mantilla R 2020 Improvement and evaluation of the Iowa Flood Center Hillslope Link Model (HLM) by calibration-free approach *J. Hydrol.* **584** 124686

Rasmussen R, Liu C, Ikeda K, Gochis D, Yates D, Chen F, Tewari M, Barlage M, Dudhia J and Yu W 2011 High-resolution coupled climate runoff simulations of seasonal snowfall over Colorado: a process study of current and warmer climate *J. Clim.* **24** 3015–48

Risser M D and Wehner M F 2017 Attributable human-induced changes in the likelihood and magnitude of the observed extreme precipitation during hurricane Harvey *Geophys. Res. Lett.* **44** 12,457–412,464

Scawthorn C *et al* 2006 HAZUS-MH flood loss estimation methodology. II. Damage and loss assessment *Nat. Hazard. Rev.* **7** 72–81

Schaller N *et al* 2016 Human influence on climate in the 2014 southern England winter floods and their impacts *Nat. Clim. Change* **6** 627–34

Schär C, Frei C, Lüthi D and Davies H C 1996 Surrogate climate-change scenarios for regional climate models *Geophys. Res. Lett.* **23** 669–72

Seo B-C, Krajewski W F, Quintero F, Elsaadani M, Goska R, Cunha L K, Dolan B, Wolff D B, Smith J A and Rutledge S A 2018 Comprehensive evaluation of the IFloodS Radar rainfall products for hydrologic applications *J. Hydrometeorol.* **19** 1793–813

Small S J, Jay L O, Mantilla R, Curtu R, Cunha L K, Fonley M and Krajewski W F 2013 An asynchronous solver for systems of ODEs linked by a directed tree structure *Adv. Water Resour.* **53** 23–32

Smith J A, Baeck M L, Villarini G, Wright D B and Krajewski W 2013 Extreme flood response: the June 2008 flooding in Iowa *J. Hydrometeorol.* **14** 1810–25

Talbot C, Bou-Zeid E and Smith J 2012 Nested mesoscale large-eddy simulations with WRF: performance in real test cases *J. Hydrometeorol.* **13** 1421–41

Van Oldenborgh G J, Van Der Wiel K, Sebastian A, Singh R, Arrighi J, Otto F, Haustein K, Li S, Vecchi G and Cullen H 2017 Attribution of extreme rainfall from Hurricane Harvey, August 2017 *Environ. Res. Lett.* **12** 124009

Wiel K V D, Kapnick S B, Oldenborgh G J V, Whan K, Philip S, Vecchi G A, Singh R K, Arrighi J and Cullen H 2017 Rapid attribution of the August 2016 flood-inducing extreme precipitation in south Louisiana to climate change *Hydrol. Earth Syst. Sci.* **21** 897–921

Yildirim E and Demir I 2019 An integrated web framework for HAZUS-MH flood loss estimation analysis *Nat. Hazards* **99** 275–86

Zhang W, Villarini G, Vecchi G A and Smith J A 2018 Urbanization exacerbated the rainfall and flooding caused by hurricane Harvey in Houston *Nature* **563** 384–8

Zogg J 2014 *The Top Five Iowa Floods* (Des Monies, IA: National Weather Service WFO)